



New daylight fluctuation control in an optical fiber-based daylighting system



A. Barbón*, A. Pardellas, J.A. Fernández-Rubiera, N. Barbón

Department of Electrical Engineering, University of Oviedo, Campus of Gijón, Spain

ARTICLE INFO

Keywords:

Daylighting system
Daylight fluctuation
Daylighting control
Solar luminaire efficiency

ABSTRACT

Daylighting systems have recently been developed as another way to harness solar energy and contribute to the reduction of greenhouse gas emissions. Various technologies can be used in daylighting systems. These technologies differ with respect to the sunlight collection systems and sunlight transmission systems they employ, but have solar luminaires in common. Many factors, such as the fluctuations in the intensity of solar irradiance, limit the efficiency of daylighting systems. This study presents the design, construction and assessment of a daylight fluctuations control for enclosed spaces with no direct access to daylight from side openings. A new control algorithm is proposed for this purpose based on daylighting monitoring and a low cost microcontroller. It also allows communication between several solar luminaires based on long range wireless solutions. The main components of the proposed daylight fluctuation control are: the luminaire, mirror, shaft, frame, stepper motor driver, stepper motor, light sensor, limit switch, XBee and microcontroller. The system uses solar luminaires and dimmable lamps. Tests performed in the laboratory on the system have shown positive results. The different dimming profiles perceived have a linear zone; hence, the perceived changes in brightness are correct. The Just Noticeable Difference is less than 200 (lx). And, the solar luminaire efficiency has good results that vary between 71.60% and 76.44%, depending on the used step angle.

1. Introduction

Different international organizations, such as the International Energy Agency (*IEA*), have compiled data on trends in energy consumption worldwide. Lighting represents about 19% of global electricity consumption [1]. This study shows that global demand for artificial light has grown over the last decade at an average rate of 2.4% per annum. It also shows that 133 petalumen-hours (*plmh*) ($1 \text{ plmh} = 1 \cdot 10^{15} \text{ lumen} \cdot \text{hours}$) of electric light were consumed in 2005 worldwide, at an average of 20 megalumen-hours (*Mlmh*) of light per person. For example, lighting is the leading energy consumer in office buildings. It represents 30% to 40% of the total energy consumption in office buildings [1]. Different strategies have been proposed to reduce the energy consumption of lighting systems [2] that can be summarized in the following points: ensuring that building codes promote the use of natural light and include minimum energy performance standards (*MEPS*) for lighting systems, as well as adopting lighting quality, reliability and *MEPS* for new and existing lighting products. The latest *IEA* estimates show that total potential energy savings in residential and services lighting could reach more than 2.4 EJ (*EJ*) per annum by 2030 [2].

Daylight-linked controls represent a very useful strategy to optimize daylighting and consequently achieve substantial energy savings [3,4].

The utilisation of daylight in buildings has been studied primarily emphasizing energy saving potentials, but the health benefits associated with the use of daylighting have been addressed in a large number of publications [5–7], the amount of illuminance and light quality being regarded as factors defining a healthy environment. However, a lack of sufficient daylight may lead to a series of symptoms such as stress, mental fatigue and seasonal affective disorder. In contrast, an excessive amount of daylight may cause discomfort glare.

Several studies have shown that daylight may affect the level of mental fatigue and stress [8]. For many people, low levels of daylight can lead to seasonal affective disorder (*SAD*) [9]. *SAD* is a mood disorder characterized by recurrent episodes of major depression occurring with a seasonal pattern [10]. Exposure to natural light has been found to be effective in the treatment of *SAD* [11].

Discomfort glare is a major problem for the daylighting design of workspaces [12]. There are empirical formulas to predict the occurrence and magnitude of discomfort glare [13]. Discomfort glare presents a continuous range of intensities, which are usually presented on numerical scales [14]. It may have effects such as headaches or posture-

* Corresponding author.

E-mail address: barbon@uniovi.es (A. Barbón).

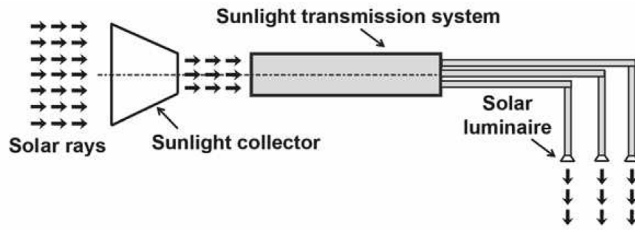


Fig. 1. Schematic of a daylighting system.

related aches after work [15].

Windows are the elements that have the most influence on the indoor environment. They provide access to daylight and hence the preference for windows is well established in the literature [16]. However, sometimes this solution is not feasible. Proximity to very high buildings and the location of workspaces in ground-floor offices usually leads to a reduction in access to daylight. This is a problem that may affect the level of mental fatigue and stress. Buildings with poor daylight illumination or a lack of it and underground railway stations have the required conditions to benefit from daylighting systems.

Daylighting systems have different components to transfer sunlight from outside the building into inside windowless spaces or even underground spaces in order to maximize electric energy savings. Their components are: sunlight sources, sunlight collection systems, sunlight transmission systems, lighting control systems and solar luminaires. Sunlight collectors capture direct sunlight outside the building, sunlight distribution systems transmit sunlight to the inside of the building and solar luminaires distribute sunlight inside the building. Fig. 1 shows a schematic diagram of a daylighting system.

There are several types of sunlight collectors: parabolic dishes, parabolic troughs, Fresnel lenses and small scale linear Fresnel reflectors. A parabolic dish system consists of mirrors collected assembled

on a supporting structure to reflect and concentrate solar radiation on the focus of the parabolic dish [17] (See Fig. 2a). In a parabolic trough system, sunlight is concentrated through a concave parabolic reflector plate into an optical fiber. The optical fiber is permanently fixed to the focus of the parabolic concentrator to collect reflected light [18] (See Fig. 2b). Fresnel lenses refract incident sunlight to a single focal point behind the opposite side of the lens, where an optical fiber bundle is mounted [19] (See Fig. 2c). Small-scale linear Fresnel reflectors use stretched rows of mirrors to focus incident solar radiation onto an optical fiber bundle that runs longitudinally above the rows of mirrors located on a common focal line of the mirrors [20] (See Fig. 2d).

Sunlight transmission systems can use several devices to transmit sunlight to the inside of buildings: large-core optical fibers, optical fiber bundles [19] and hollow-core reflective light-pipes [21]. The transmission of sunlight via optical fiber is a flexible solution for daylighting systems and has some advantages such as the exclusion of the ultraviolet rays and, more importantly, infrared rays.

Sunlight propagation inside an optical fiber is unidirectional and can be described using skew and meridional rays [22]. Due to the unidirectional propagation of sunlight propagation, the system for illuminating a workspace is designed in such a way that each optical fiber bundle behind an optical element will diffuse the sunlight at a uniform illumination level (See Fig. 3). This type of system is efficient, as all emitted sunlight is directly focused onto the work surface. Therefore, a solar luminaire is an optical element designed to diffuse sunlight emitted from an optical fiber bundle with a uniform illuminance level on the working plane. Solar luminaires constitute sensitive elements in daylighting systems as the effective use of natural light inside buildings depends on them. The main characteristics that solar luminaires have to fulfill are those of [24]: (i) maximizing the use of available light, (ii) minimizing glare, and (iii) providing uniform steady illuminance levels on the work surface. Solar luminaires may be classified as passive or hybrid. Passive solar luminaires are designed to be

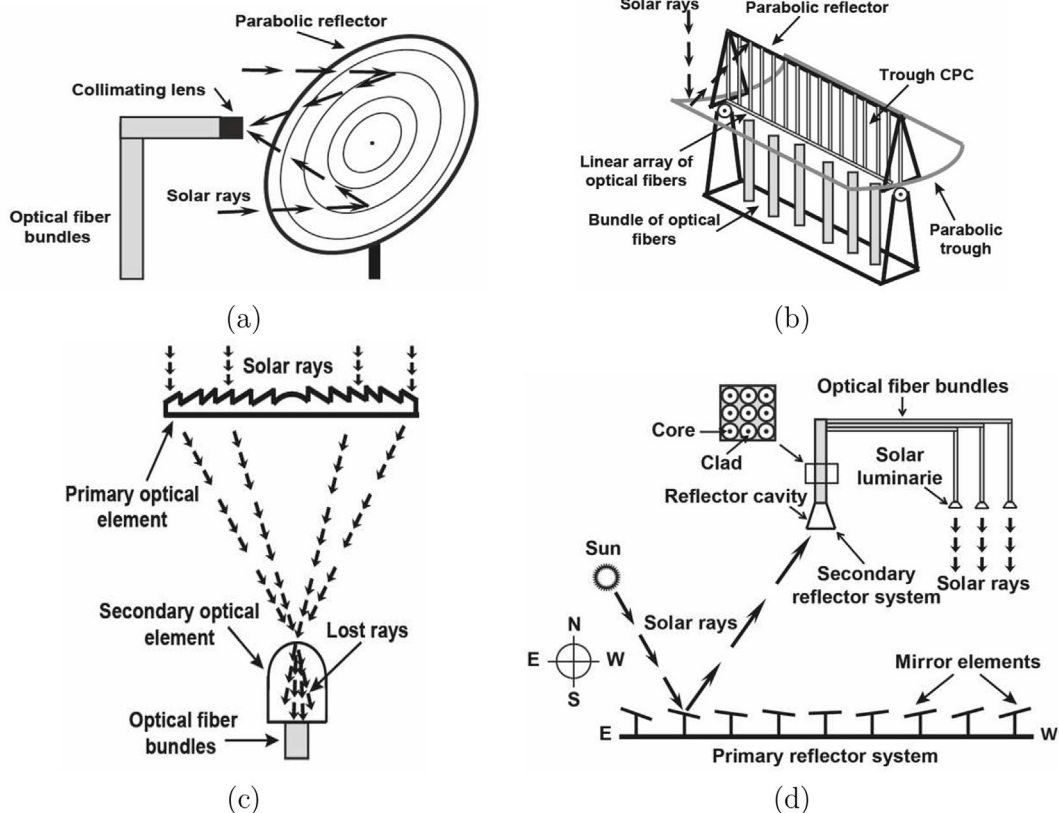


Fig. 2. Types of sunlight collectors.

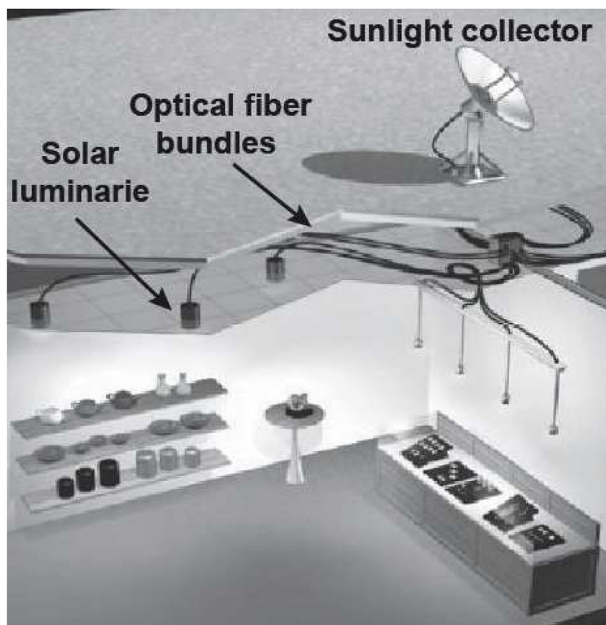


Fig. 3. Conceptual illustration of an optical fiber-based daylighting system [23].

used only when adequate direct sunlight can be collected. Hybrid solar luminaires are designed to be used continuously regardless of the presence of direct sunlight, as they are associated with dimmable electric lamps and a light sensor. A solar luminaire is made of materials such as purified silica glass or a synthetic polymer called Polymethyl methacrylate or *PMMA*. The efficiency of this system can be around 80% [25].

As the very high intensity of collected sunlight can cause discomfort glare, the main objective of this paper is to design an automatic control system capable of rapidly adjusting the high intensity of collected sunlight. Furthermore, as a low intensity of collected sunlight can cause insufficient illumination, this paper also aims to supplement natural light with electric lamps. If the electric light levels continuously change to adapt themselves to daylight variations, also can cause discomfort glare. The low cost of the proposed control system is another of the goals of the study. The performance of the daylight fluctuation control has been analyzed through laboratory tests in order to evaluate its efficiency.

The paper is organized as follows. The statement of the problem, the elements, the implementation, and the algorithms are presented in Section 2. Section 3 presents the results of the study, while Section 4 summarizes the main contributions and conclusions of the paper.

2. Materials and methods

2.1. Problem statement

Various daylight-linked control technologies have been developed to utilize daylight as an additional light source in indoor space. The types of daylight-linked control are [26]: daylight-linked switching and daylight-linked dimming. In the former, the electric lights are controlled by switching between ‘on’ and ‘off’ according to the available daylight. In the latter, a dimming system continuously controls the electric lamp output using a dimmable electronic ballast. Various studies have analyzed the daylight fluctuations and the effects on the functioning of different daylight-linked control systems [27,28]. Electric light fluctuations due to daylight variability are especially problematic when switching systems are installed [27].

The intensity of collected sunlight changes systematically, the most rapid changes occurring during twilight. The intensity decreases as

dusk falls and increases as dawn breaks as a function of the height of the Sun. These fluctuations in the intensity of collected sunlight can cause glare, insufficient light and non-uniformity in illuminance levels. These daylight fluctuations are caused by variations of the cloud cover or by movement of the solar collector.

The variability in solar radiation and irradiance transitions caused by the shadows of moving clouds are essential parameters in determining the response time required by the system. These parameters have been studied, for example, in Refs. [32,33]. The apparent velocity of clouds produces falls and rises in irradiance on the solar collector. Lappalainen et al. [34] shows that the average speed is 8.7 and 8.4 (*m/s*) for the falls and the rises, respectively. The lengths of irradiance transitions caused by the edges of moving clouds are typically around 100 (*m*) [34]. Therefore, the average angular velocity of the clouds, with regard to the solar luminaire, is 0.087 and 0.084 (*rad/s*) for falls and the rises, respectively.

These daylight fluctuations can be produced by a high or low intensity of collected sunlight. The proposed system solves this problem in two different ways: it will reduce the intensity of collected sunlight by driving a stepper motor when the intensity of collected sunlight is very high, and will supplement natural light with an electric lamp when the intensity of collected sunlight decreases. A good lighting control must quickly compensate these fluctuations, maintaining a constant level of illuminance [35].

Previous studies have analyzed the factors influencing occupant visual comfort:

- (i) The human eye is less sensitive to extremely gradual changes and is fairly sensitive to more rapid changes [36].
- (ii) The human eye is able to continuously adapt itself to the change of light, but a repeated change of light within a short interval causes eye fatigue and visual discomfort [28].

The time between two consecutive daylight adjustments and the fluctuation entity [28], are two factors that need to be taken into account in the design of the control system.

Hence, the aim of this study is to design a daylight fluctuations control capable of gradually compensating the variability in solar radiation and irradiance transitions.

2.2. Elements of the daylight fluctuations control

A hybrid lighting system comprises a combination of electrical and natural light sources at each individual workstation. The system has to be able to produce a uniform source of light using natural light, electrical light, or both sources. This control system is developed to ensure that the combination of daylighting and electrical lighting maintains a steady lighting level.

The main components of the proposed daylight fluctuations control are: the luminaire, mirror, shaft, frame, stepper motor driver, stepper motor, light sensor, limit switch, XBee and microcontroller. The mirror is mounted on a frame made of a thermoplastic material, being fixed on the frame using an industrial adhesive. The frame was manufactured using a 3D printer. The rotation shaft comprises a carbon steel bar. All these elements are located on the ceiling. The structure of the newly developed solar luminaire control is shown in Fig. 4. The sunlight transmitted via optical fiber is reflected onto a mirror. This mirror is rotated between 0 and 90° by means of a stepper motor. This direct solar radiation is directed to the light dispersion element so as to distribute the light evenly. The stepper motor driver can adjust the natural illumination level. The dimmable electronic ballast can adjust the artificial illumination level in the presence or absence of natural light. The luminaire is a diffuser, similar in shape to a downlight.

This control system can be integrated in a smart lighting system in which several solar luminaires are used. For this reason, a wireless technology solution is chosen as a connectivity option.

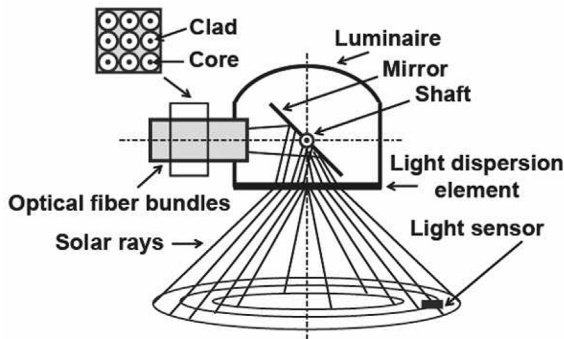


Fig. 4. Schematic of a solar luminaire control.

Fig. 5 shows several photographs of the prototype.

2.3. Hardware specification

The proposed daylight fluctuations control has been conceived as a combined architecture embedding sensing elements (light sensor, limit switch) and actuators (stepper motor drive, electronic dimmable ballast) that are managed by a dedicated control unit. This control unit is implemented by means of a microcontroller. The microcontroller has the following functions: to collect data from sensors (light sensor, limit switch), to drive actuators (stepper motor drive, electronic dimmable ballast) and to transfer information (*XBee*).

The daylight fluctuations control continuously monitors the level of light (light sensor), which includes light from both the daylight source and an electric lamp. The changes in the light level of the electric lamp due to fluctuations in the intensity of collected sunlight are continuously transmitted to the control system.

Fig. 6 provides photographs of the hardware specification of the daylight fluctuations control.

2.3.1. Microcontroller

The daylight fluctuations control is based on an Arduino Mini [29]. The Arduino Mini is used because of its low cost, compact size, compatibility and easy interfacing. The Arduino Mini is a small microcontroller board based on the ATmega 328. It has 14 digital input/output pins (6 of which can be used as PWM outputs), 8 analog inputs and a 16 MHz crystal oscillator. It can be programmed using the USB Serial adapter or another *USB* or *RS232* to *TTL* serial adapter. The Arduino Mini has the following inputs: light sensor and limit switch; and the following outputs: stepper motor driver, electronic dimmable ballast and *Xbee*.

2.3.2. Light sensor

The task of the light sensor is to maintain the lamp at a certain illuminance level at each individual workstation. A *BH1750* can be used for this purpose. This sensor is an ambient light intensity sensor. The breakout board has a built-in 16-bit A2D converter that can directly provide a digital output signal. The output from the sensor is in Lux (*Lx*) and does not require advanced calculations in the sketch. The *BH1750* communicates using the *I²C* Protocol. It is possible to detect a wide range at High resolution ($1 - 65535 \text{ lx}$). The resolution is a 1 (lx) . The light sensor has three terminals, V_{DC} , ground and output signal. Its features are: power supply $V_{DC \text{ max}} = 4.5 \text{ (V)}$, current supply $I_{\text{max}} = 7 \text{ (mA)}$.

2.3.3. Limit switch

Its features are: power supply $V_{AC \text{ max}} = 250 \text{ (V)}$, current supply $I_{\text{max}} = 15 \text{ (A)}$.

2.3.4. Stepper motor

A stepper motor with the step angle variable has been used. The stepper motor is a *28BYJ - 48 - 5V*. The *28BYJ - 48* is a small, low-cost stepper motor suitable for a large range of applications. Its features are: power supply $V = 5 \text{ (V)}$, current supply $I = 83 \text{ (mA)}$.

2.3.5. Stepper motor driver

One stepper motor driver is dedicated to the sole stepper motor. The driver supplies appropriate control signals and supply voltage to the associated step motor, so that the step motor rotates in the appropriate direction (clockwise direction or anticlockwise direction) and the number of steps requested by the microcontroller. The step motor driver is a *ULN2003*.

2.3.6. XBee

There are various connectivity solutions for a smart lighting system. Wireless networks are usually preferred. The most popular wireless technologies used are Wi-Fi, Bluetooth and ZigBee. ZigBee is usually preferred due to its low cost and low power consumption.

The *XBee* module is a technology for wireless communication among multiple devices in a Wireless Personal Area Network. *XBee* modules are embedded solutions that provide wireless end-point connectivity to devices. This module is a standard for wireless communication based on the *IEEE802.15.4* protocol. The *XBee* module is equipped with an on-chip antenna provided by Digi-MaxStream [30]. The transmission capabilities (ranges, consumption, etc.) are shown in Ref. [30]. These transmission capabilities have been widely tested and provide optimal performances [31].

2.3.7. DC-to-DC converter

The electronic dimmable ballast has input voltage values of ($1 - 10V_{DC}$). A *PWM* output of the Arduino Mini ($0 - 5V_{DC}$) and a DC-to-DC converter are used to obtain this power range.

2.3.8. Cost analysis

The total cost of the implemented daylight fluctuations control with an integrated controller and wireless module is calculated and presented in Table 1. The cost of the microcontroller, integrated sensors and stepper motor is 18.51% of the overall cost of the system. The cost of the downlight, mirror and shaft subassembly is 28.42% of the total cost of the system. The cost of the wireless module is 40.49% of the total cost of the system. The wireless module represents a high percentage of the total cost. This module could be removed when the solar luminaire works autonomously. Should this be the case, data on the solar luminaire would no longer be necessary.

2.4. Daylight fluctuation control algorithms

The algorithm has to fulfil the following conditions:

- (i) If the light level is higher than the predefined value, the stepper motor starts to rotate to reduce the natural light level and the electric lamp is turned off.
- (ii) If the light level is lower than the predefined value, the electric lamp is controlled according to the availability of daylight in order to supplement natural light during cloudy periods.

The algorithm is shown in Fig. 7. The following is an analysis of each of the blocks.

2.4.1. Mirror movement control

The position of the mirror can be adjusted using two movements. Therefore, a stepper motor and stepper motor driver are used for the movements of the mirror. The stepper motor can adjust the level of natural illumination. The driver supplies appropriate control signals and supply voltage to the associated stepper motor. The microcontroller

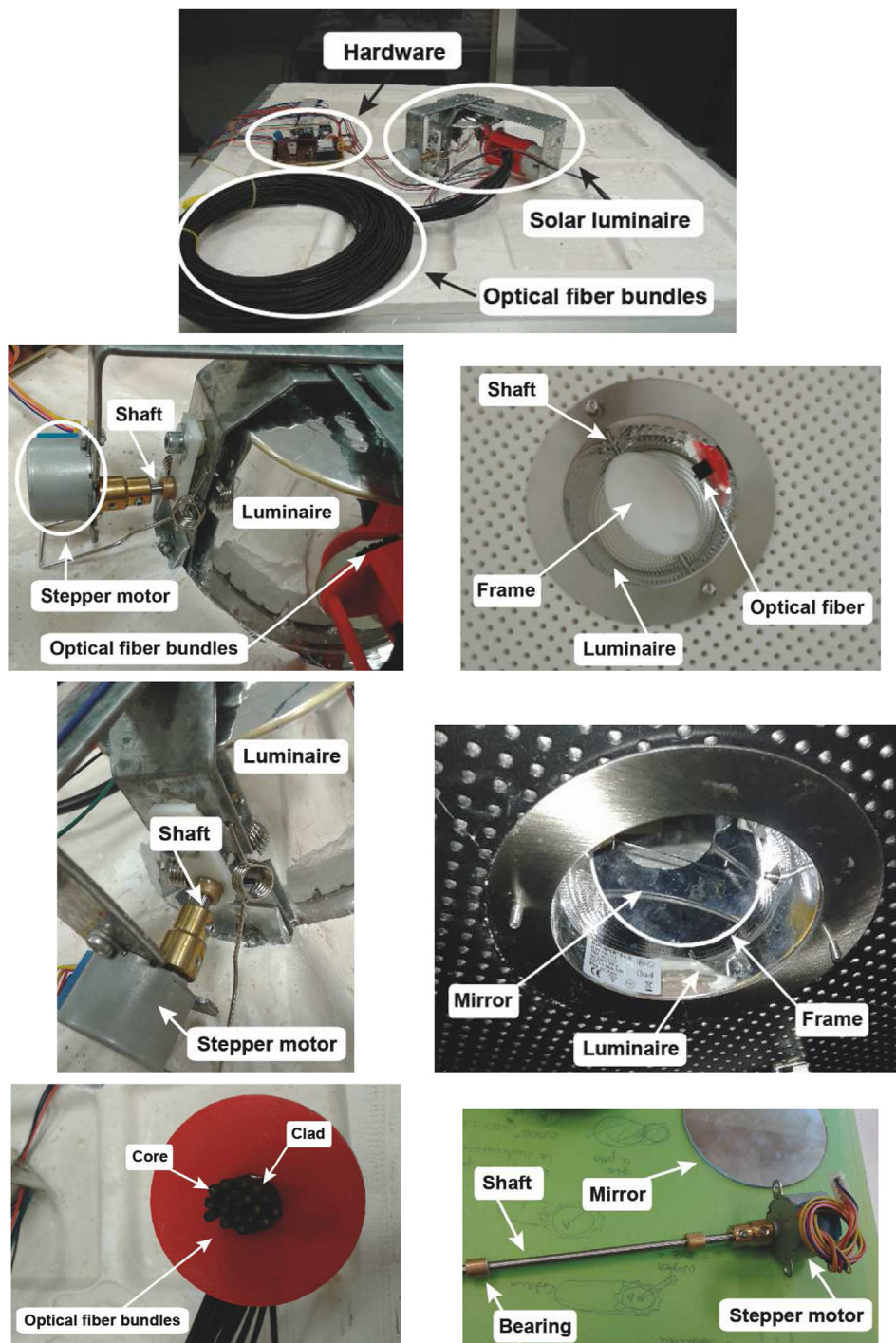


Fig. 5. Photographs of the prototype.

is responsible for the stepper motor, which rotates according to the required direction and stepping number. The stepper motor motion is described as follows:

- (i) If the light level is higher than the predefined value, the stepper motor begins to run clockwise. Thus, the mirror is driven step by step in the clockwise direction. With the increase in the step number, the light level decreases.
- (ii) After a while, the current value is compared again to the previous value of the light level. If this new value is still higher than the previous one, the stepper motor continues to run clockwise.
- (iii) When this condition is no longer fulfilled, the stepper motor begins

to run anticlockwise. Thus, the mirror is driven step by step in the anticlockwise direction. The stepper motor will stop at the starting position.

The algorithm can be seen in Fig. 8.

2.4.2. Initial mirror position

The initial position of the mirror is the position in which the system delivers the highest amount of solar luminous flux. In this position, the mirror forms a certain angle with a horizontal plane. This angle is shown in Section 3. This position is determined by a limit switch. The stepper motor motion is described as follows: if the limit switch signal is

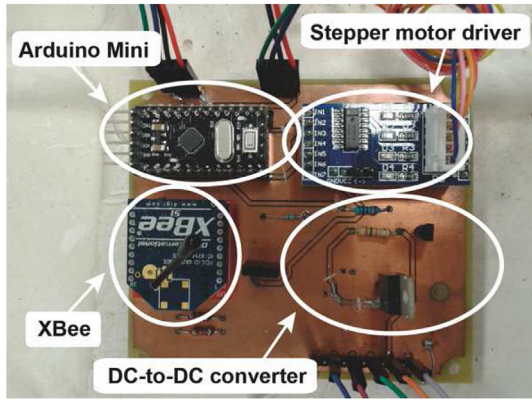


Fig. 6. Photographs of the hardware prototype.

Table 1
Cost of the daylight fluctuations control.

Item	Unit cost (€)	Quantity	Cost (€)
Arduino mini pro	3.25	1	3.25
Light sensor (BH1750)	2.90	1	2.90
Limit switch	0.20	1	0.20
4K7 resistor	0.20	2	0.40
7K5 resistor	0.15	1	0.15
10K resistor	0.1	1	0.1
1K resistor	0.05	1	0.05
ka7810 voltage regulator	0.13	1	0.13
BC639 transistor	0.03	1	0.03
0.33 μF capacitor	0.5	1	0.5
0.1 μF capacitor	0.8	1	0.8
28BYJ-48-5V Stepper motor + ULN2003	1.60	1	1.60
XBee module S1	16.95	1	16.95
Mirror	0.9	1	0.9
Shaft + frame	5	1	5
Downlight	6	1	6
PCB cost	2.9	1	2.9
Total			41.86

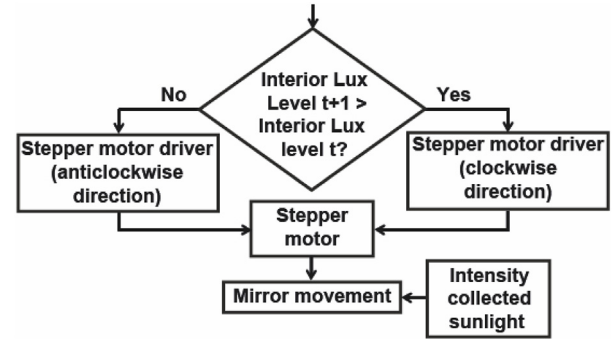


Fig. 8. Control algorithm of the mirror movement control.

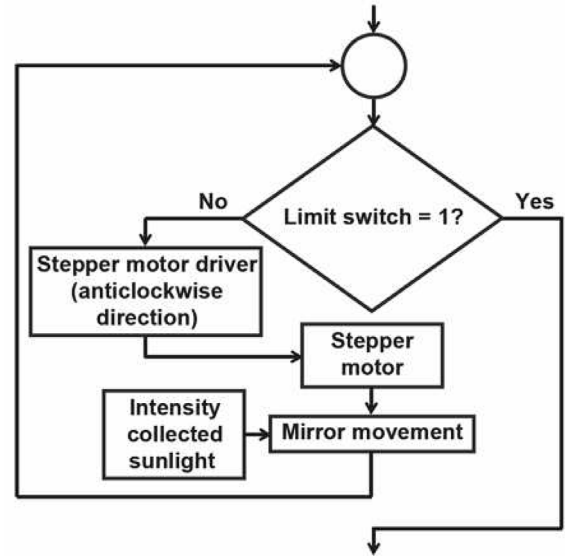


Fig. 9. Control algorithm of the initial mirror position.

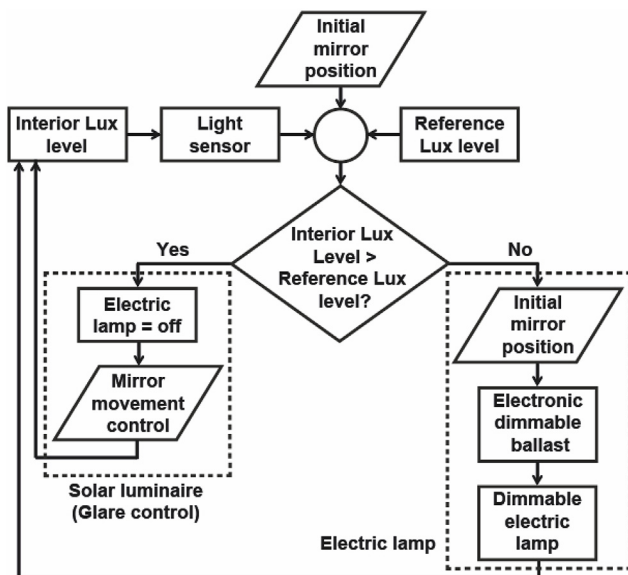


Fig. 7. Control algorithm of the proposed hybrid lighting system.

not equal to 1, the stepper motor begins to run anticlockwise. Thus, the mirror is driven step by step in the anticlockwise direction until the limit switch signal is equal to 1. The algorithm is shown in Fig. 9.

2.5. Electric lamp control

The dimmable electric lamp can be used with dimmable electronic circuits to provide artificial light when daylight is insufficient. The type of electric lamp control is a closed loop (See Fig. 7). The change in the light levels of the lamp due to the availability of daylight is continuously feeding the control system and it can make the necessary adjustments.

3. Results and discussion

3.1. Experimental analyses

The purpose of this experimental phase, carried out in the laboratory, was to verify the feasibility and applicability of the proposed daylight fluctuations control. The experiment was conducted in a test box in order to measure the illuminance values provided by the hybrid lighting system. The test box is a pre-fabricated box measuring 575 (mm) long, 575 (mm) wide and 498 (mm) in height. In order to avoid reflection from the inner walls of the test box, all its surfaces were covered with black matte fabric with a reflectance value lower than 0.1. The ceiling of the test box was painted black, with a matte paint with a reflectance value of approximately 0.1. The zero illuminance value inside the test box was verified in order to obtain precise measurements with the solar luminaire and the electric lamp. Illuminance values were measured by a light sensor, the characteristics of which are summarized in this section. The solar luminaire and electric lamp were mounted in the upper part of the test box, while the light sensor was placed at the

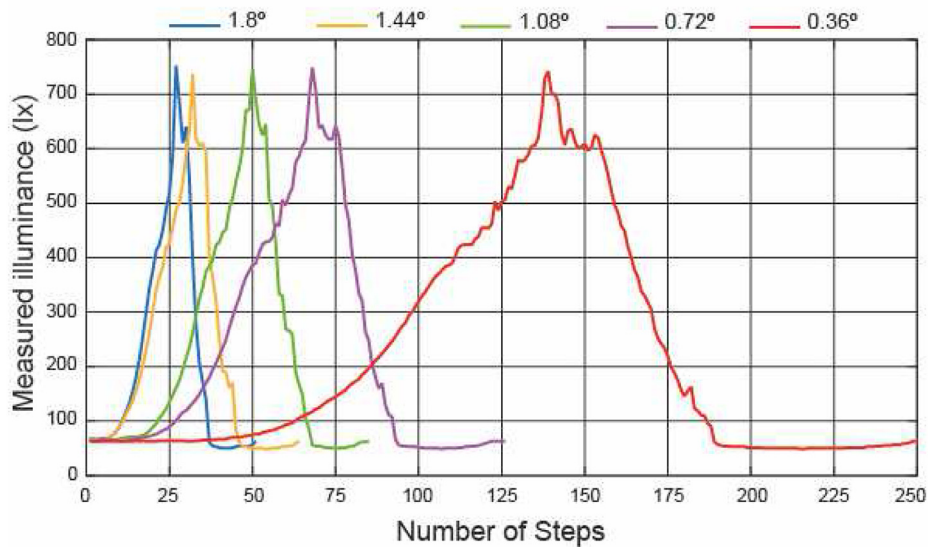


Fig. 10. Relationship between illuminance values and number of steps.

bottom. The horizontal distance between the light sensor and the center of the diffuser is 175 (mm), approximately.

A portable fiber optic light source was used in all the experimental tests. Different step angles were employed for each test.

Problems with this daylight fluctuations control occur when the intensity of collected sunlight is very high. In this case, the amount of light emitted by the solar luminaire needs to be reduced. Fig. 7 shows the different illuminance values, obtained with a constant luminous flux, for different step angles (1.80°, 1.44°, 1.08°, 0.72°, 0.36°) of the stepper motor. Some precision motors are able to make 1000 steps in one revolution, with a step angle of 0.36°. A standard motor will have a step angle of 1.8°, with 200 steps per revolution. The initial mirror position corresponds to the maximum illuminance value.

Each time a command pulse is received, one step is taken. This value is 1 s which is enough time for the microcontroller to respond to irradiance transitions. The duration of irradiance transitions varies a lot, from 1 s up to several minutes [32].

Each graph in Fig. 10 is composed of two sides, separated by the maximum illuminance value. On the left side of the graph, the position of the mirror varies from 0° to the initial mirror position. Conversely, on the right side of the graph, the position of the mirror varies from the initial mirror position up to 90°. Each of these sides has different slopes. The slope of the left side of the graph is lower, so the variation of the illuminance will be more gradual. Obviously, the more the step angle decreases, the more the slope decreases.

Our dimming profile is the relationship between the daylight output level (in percentage values with respect to the illuminance of the initial mirror position) and the mirror position (in percentage values with respect to the initial mirror position). To obtain the dimming profile of each side of the curve, the values have been adjusted to a 2nd-order polynomial. Table 2 shows the values of R². The best results are obtained with the left side of the graph. Fig. 11 shows the dimming profiles for the left side.

Table 2
Values of R² for the dimming profiles.

Step angle (°)	Left side	Right side
1.80	0.9921	0.9794
1.44	0.9960	0.9863
1.08	0.9967	0.9942
0.72	0.9958	0.9877
0.36	0.9968	0.9848

An artificial lighting system consists of a dimmer, a driver and a luminaire. The combination of dimmer and driver is different in the workings of the human eye. The human eye does not perceive changes in light level in a linear manner. Human vision operates according to a logarithmic function [38], which can be approximated to a square function [39]. The perceived brightness is approximated by the following equation:

$$\text{Perceived Brightness} \approx \sqrt[3]{\text{Measured Brightness}} \tag{1}$$

The aim is to achieve a perceived linear dimming, so that the perceived changes in brightness may be discerned. In other words, the brightness of the light must be matched to the way our eyes behave. To obtain the perceived dimming profiles, the dimming profiles are used in conjunction with equation (1). Fig. 12 shows the comparison between dimming profiles.

Fig. 13 shows the different dimming profiles perceived for different step angles (left side). As shown in this figure, all dimming profiles perceived have a linear zone, which is curved as the mirror position decreases.

Human eye is less sensitive to extremely gradual changes. Table 3 shows the number of steps in the linear zone for each dimming profile perceived (left and right side).

Another indicator that has been considered is the Just Noticeable Difference (JND). The JND is the illuminance difference of a given target under given viewing conditions that the average observer can just perceive. The total JND steps for the eye is about 1000, while the total JND steps for fixed adaptation is about 200 [40]. Table 4 shows the maximum JND.

Several studies have demonstrated that occupants prefer to have control over lighting [41,42]. This is because the visual comfort of each occupant depends on “human factors” [43]. Therefore, the choice of the suitable step angle is subjective, being an appreciation of the occupant. From the point of view of gradual changes, a step angle of 0.36° is the best. From the point of view of the JND, all the step angles are below 200 (lx).

3.2. Solar luminaire efficiency

The daylight output of a solar luminaire is a function of the luminous flux produced by the optical fiber bundles and the solar luminaire efficiency. Solar luminaire efficiency (η_{SL}) is the ratio of light output emitted by the solar luminaire to the light output emitted by its optical fiber bundles. Solar luminaire efficiency is given by:

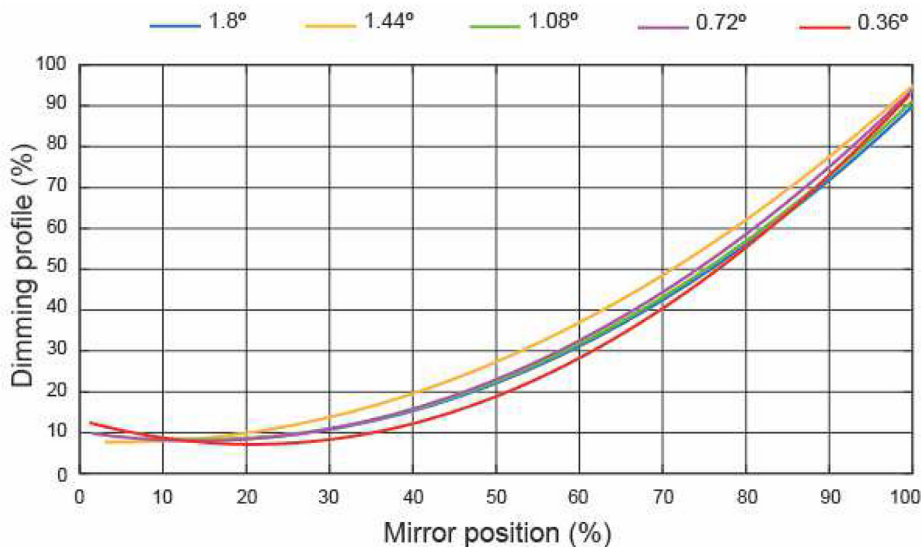


Fig. 11. Dimming profiles for different step angles (Left side).

$$\eta_{SL} = \rho_m \cdot CI_m \cdot CI_d \cdot \tau_d \cdot (C_1 \cdot n^2 + C_2 \cdot n + C_3) \tag{2}$$

Where ρ_m is the reflectivity of the mirror, CI_m is the cleanliness factors of the mirror, CI_d is the cleanliness factors of the diffuser, τ_d is the transmissivity of the diffuser, n is the number of steps, and C_1, C_2, C_3 are coefficients of the 2nd-order polynomial that adjusts to the dimming profile. These values are: $\rho_m = 0.94$ (see Ref. [44]); $CI_m = CI_d = 0.96$ (see Ref. [45]); $\tau_d = 0.92$ for Polymethyl methacrylate, taken from manufacturer data [46]. Table 5 shows the coefficients $C_1, C_2,$ and C_3 (dimming profile of left side).

Table 6 shows the solar luminaire efficiency for the initial mirror position.

A typical workstation was considered in order to evaluate the solar luminaire efficiency of a daylighting system. The workstation characteristics are summarized in Table 7. The luminous flux delivered was calculated using the lumen method. The characteristics of an optical fiber daylighting system based on a small scale linear Fresnel reflector are summarized in Table 8. Meteorological database [51] have been used to estimate the solar irradiance.

Fig. 14 shows the simulation results using Matlab code to evaluate the solar luminaire efficiency, for Summer solstice (June 21st), Winter solstice (December 21st), March equinox (March 21st) and September equinox (September 21st). At Winter solstice, the mirror is always placed at its initial position, for that reason, the solar luminaire efficiency keeps at a constant value. During all the other days we have studied, the solar luminaire efficiency gradually varies its value. The higher the light output emitted by the optical fiber bundles, the smaller the solar luminaire efficiency which is the aim of this paper.

Fig. 15 shows the luminous flux of the solar luminaires, for Summer solstice, Winter solstice, March equinox and September equinox. These figures represent the luminous flux output emitted by the solar luminaires (Out solar luminaires), the luminous flux output emitted by the optical fiber bundles (In solar luminaires), and the luminous flux required for the current study.

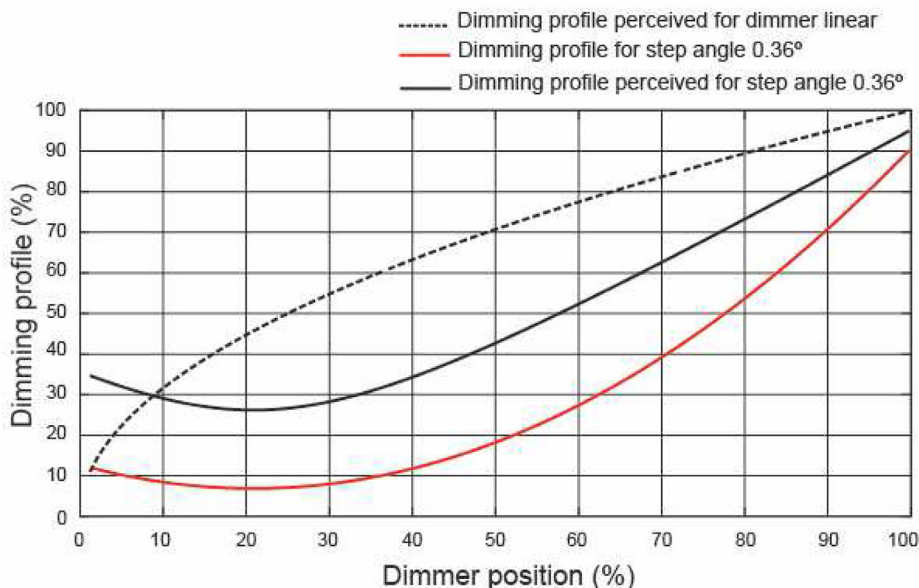


Fig. 12. Dimming profiles comparison.

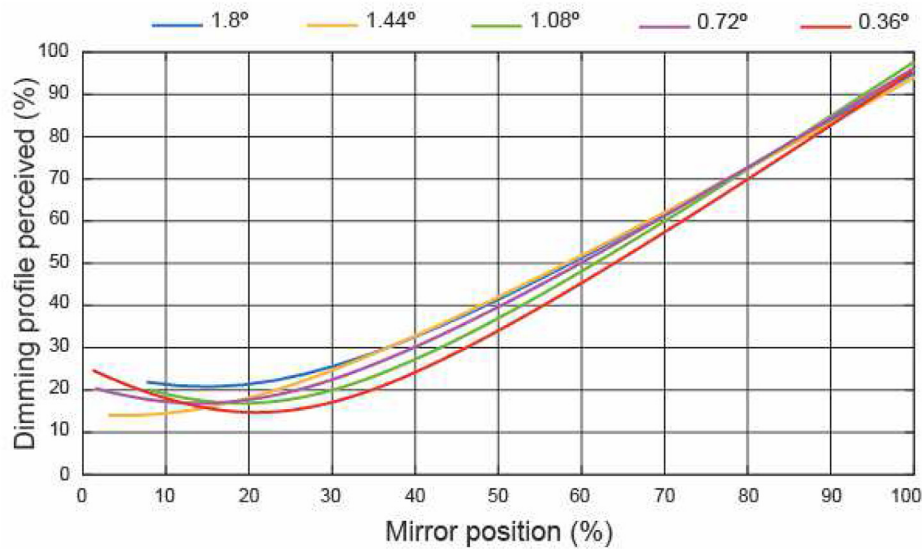


Fig. 13. Different dimming profiles perceived.

Table 3
Number of steps in dimming profile perceived with a linear dimming range.

Step angle (°)	Left side	Right side
1.80	10	7
1.44	12	8
1.08	19	10
0.72	24	18
0.36	59	33

Table 4
Maximum just noticeable difference.

Step angle (°)	JND (lx)	
	Left side	Right side
1.80	165	149
1.44	102	196
1.08	75	138
0.72	75	69
0.36	65	58

Table 5
Coefficients C_1 , C_2 , and C_3 .

Step angle (°)	C_1	C_2	C_3
1.80	0.000513565	- 0.007113163	0.106406215
1.44	0.000480007	- 0.002149688	0.079167717
1.08	0.000480134	- 0.009712789	0.128576076
0.72	0.000489261	- 0.00662717	0.100161939
0.36	0.000070261	- 0.004046023	0.126817494

Table 6
Initial mirror position values.

Step angle (°)	Solar luminaire efficiency	n
1.80	0.7160	26
1.44	0.7489	31
1.08	0.7644	49
0.72	0.7324	67
0.36	0.7225	138

Table 7
Data from the workstation object of study.

Data	Value
Geographic location	Almeria (Spain)
Latitude	36°50'07" N
Longitude	02°24'08" W
Altitude	22 (m)
Workstation dimension (L x W x H)	4 (m) x 4 (m) x 3 (m)
Workstation reflectance ($\rho_{ceiling} \times \rho_{wall} \times \rho_{floor}$)	0.5 x 0.5 x 0.2
Other object reflectance	1.0
Height of working plane from floor	0.85 (m)
Maintenance factor	0.8
Utilisation factor	0.44
Average illumination level [47]	500 (lx)
Office working hours	09: 00 to 16: 30

Table 8
Data from the fiber daylighting system used in the study.

Parameters	Value
Number of mirrors at each side of the central mirror	12 [20]
Mirror width	0.03(m) [20]
Separation between two consecutive mirrors	0.022 (m) [20]
Height of the receiver	1.5 (m) [20]
Mirror length	2.5 (m) [20]
Luminous efficacy	$K_b = 104 (lm/W)$ [48,49]
Attenuation at each wavelength	12 (dB/Km) [50]
Bundle packing fraction	40% [20]
Length of the individual optical fiber	0.010 (Km)
Number of solar luminaires	16
Step angle	0.36°
Fluorescent lamp	1350 (Lm)
Number of fluorescent lamps	16

4. Conclusions

This paper presents a new daylight fluctuations control especially conceived for enclosed spaces with no access to daylight from side openings. When the intensity of solar irradiance is very high the different daylight-linked control systems are not valid. This system is based on a low cost microcontroller. It also allows communication between each solar luminaire and a main controller. This communication is based on a long-range wireless solution. Therefore, this control system can be integrated in a smart lighting system in which several

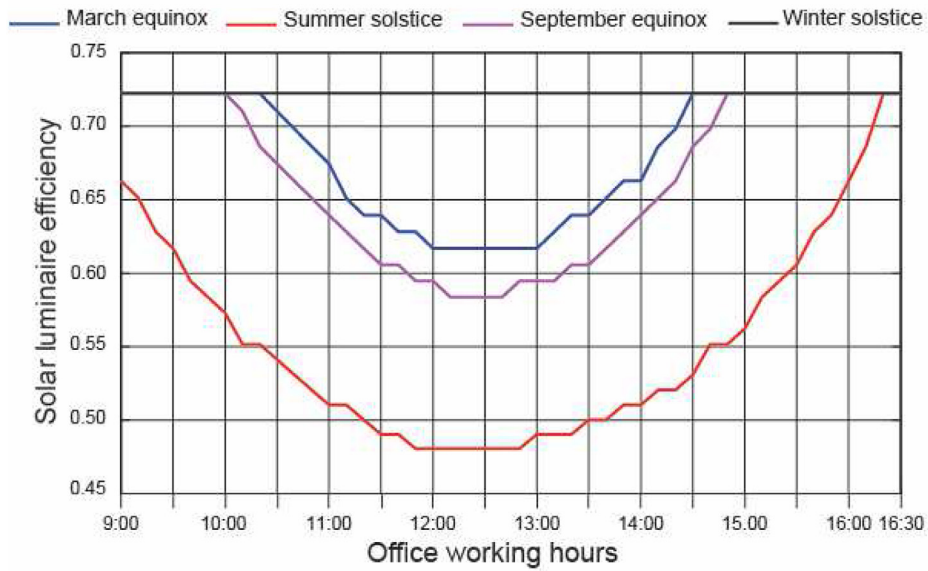
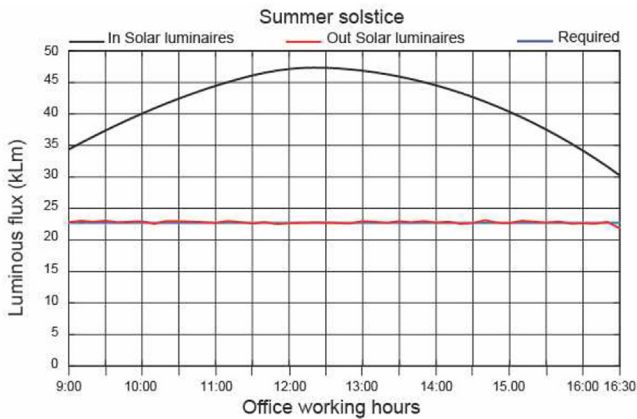


Fig. 14. Solar luminaire efficiency.

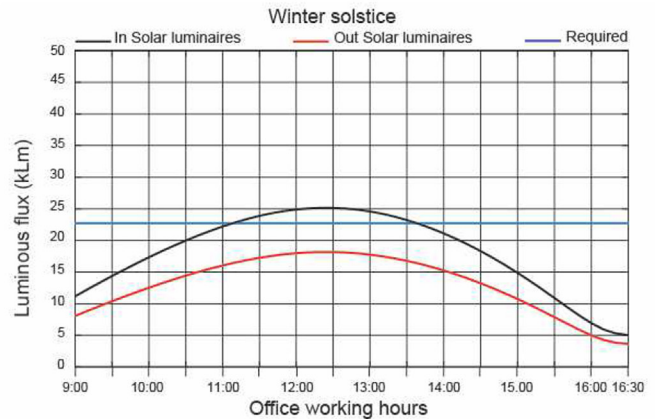
solar luminaires are used.

Laboratory tests on the daylight fluctuations control have shown positive results. At the end of the experimental laboratory tests, the main results comprise: (i) its functionality and applicability to real cases; (ii) its low cost; (iii) the fact that its different dimming profiles,

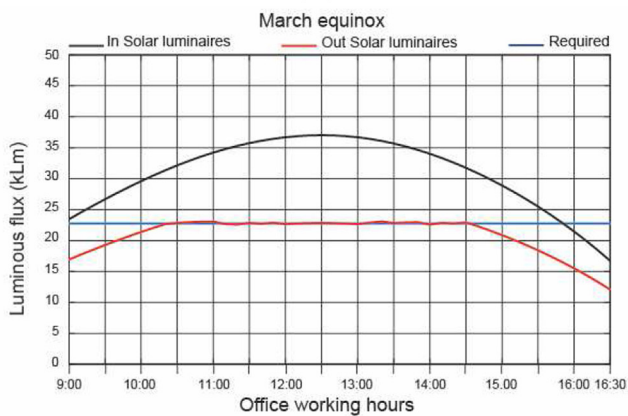
perceived with different step angles, have a linear zone, as a result of which the perceived changes in brightness are correct; (iv) the fact that, for gradual changes, a step angle of 0.36° is the best; (v) The solar luminaire efficiency, at the initial mirror position, has good results for all step angles, but its best results are obtained with a step angle of 1.08° ;



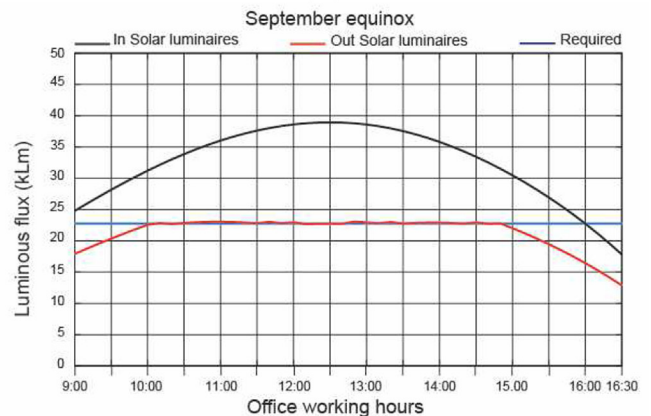
(a)



(b)



(c)



(d)

Fig. 15. Luminous flux.

and (vi) its Just Noticeable Difference is less than 200 (lx) for any step angle used.

With regard to possible future work, the possibility exists of studying the use of this daylight fluctuations control integrated in a smart lighting system in applications such as multi-floor office buildings or underground railway stations, among others.

References

- [1] I.E.A. Light's, labour's Lost. Policies for Energy-Efficient Lighting, International Energy Agency, 2006.
- [2] IEA, 25 Energy Efficiency Policy, International Energy Agency, 2011.
- [3] J. Snyder, Energy-saving strategies for luminaire-level lighting controls, *Build. Environ.* (2018), <https://doi.org/10.1016/j.buildenv.2018.10.026>.
- [4] P. Ihm, A. Nemri, M. Krarti, Estimation of lighting energy savings from daylighting, *Build. Environ.* 44 (2009) 509–514.
- [5] J. Hraska, Chronobiological aspects of green buildings daylighting, *Renew. Energy* 73 (2015) 109–114.
- [6] G. Kim, J.T. Kim, Healthy-daylighting design for the living environment in apartments in Korea, *Build. Environ.* 45 (2010) 287–294.
- [7] P. Boyce, C. Hunter, O. Howlett, The Benefits of Daylight through Windows, Lighting Research Center: Rensselaer Polytechnic Institute, New York, 2003.
- [8] D. Li, W.C. Sullivan, Impact of views to school landscapes on recovery from stress and mental fatigue, *Landsc. Urban Plann.* 148 (2016) 149–158.
- [9] C. Sarrana, C. Albers, P. Sachona, Y. Meesters, Meteorological analysis of symptom data for people with seasonal affective disorder, *Psychiatr. Res.* 257 (2017) 501–505.
- [10] American Psychiatric Association, Depressive disorders, Diagnostic and Statistical Manual of Mental Disorders DSM-5, fifth ed., American Psychiatric Association, Arlington, Va, 2013, <http://www.psychiatryonline.org>, Accessed date: 6 June 2018.
- [11] A. Wirz-Justice, P. Graw, K. Kräuchi, A. Sarrafzadeh, J. Engh, J. Arendt, L. Sand, Natural light treatment of seasonal affective disorder, *J. Affect. Disord.* 37 (1996) 109–120.
- [12] R.D. Clear, Discomfort glare: what do we actually know? *Light. Res. Technol.* 45 (2) (2013) 141–158.
- [13] S. Carlucci, F. Causone, F. De Rosa, L. Pagliano, A review of indices for assessing visual comfort with a view to their use in optimization processes to support building integrated design, *Renew. Sustain. Energy Rev.* 47 (2015) 1016–1033.
- [14] Y. Bian, T. Leng, Y. Ma, A proposed discomfort glare evaluation method based on the concept of 'adaptive zone', *Build. Environ.* 143 (2018) 306–317.
- [15] R.G. Rodríguez, J.A. Yamín, A.E. Pattini, An epidemiological approach to daylight discomfort glare, *Build. Environ.* 113 (2017) 39–48.
- [16] M.B.C. Aries, *Human Lighting Demands : Healthy Lighting in an Office Environment*, Technische Universiteit Eindhoven, Eindhoven, 2005, <https://doi.org/10.6100/IR594257>.
- [17] L. Sedki, M. Maaroufi, Design of parabolic solar daylighting systems based on fiber optic wires: a new heat filtering device, *Energy Build.* 152 (2017) 434–441.
- [18] I. Ullah, S. Shin, Highly concentrated optical fiber-based daylighting systems for multi-floor office buildings, *Energy Build.* 72 (2014) 246–261.
- [19] I. Ullah, H. Lv, A.J.-W. Whang, Y. Su, Analysis of a novel design of uniformly illumination for Fresnel lens-based optical fiber daylighting system, *Energy Build.* 154 (2017) 19–29.
- [20] A. Barbón, J.A. Sánchez-Rodríguez, L. Bayón, N. Barbón, Development of a fiber daylighting system based on a small scale linear Fresnel reflector: theoretical elements, *Appl. Energy* 212 (2018) 733–745.
- [21] D. Jenkins, T. Muneer, Modelling light-pipe performances-a natural daylighting solution, *Build. Environ.* 38 (2003) 965–972.
- [22] M. Tekelioglu, B.D. Wood, Solar light transmission of polymer optical fibers, *Sol. Energy* 83 (2009) 2039–2049.
- [23] Hybrid Solar Lighting Illuminates Energy Savings for Government Facilities, U.S. Department of Energy, Energy Efficiency and Renewable Energy, DOE/EE-0315, 2007.
- [24] D.D. Earl, J.D. Muhs, Preliminary results on luminaire designs for hybrid solar lighting systems, Presented at the American Society of Mechanical Engineers, Forum 2001: Solar Energy, Washington, D.C, 2001.
- [25] A.A. Earp, G.B. Smith, J. Franklin, P. Swift, Optimisation of a three-colour luminescent solar concentrator daylighting system, *Sol. Energy Mater. Sol. Cells* 84 (2004) 411–426.
- [26] M.A. Haq, M.Y. Hassan, H. Abdullah, H.A. Rahman, M.P. Abdullah, F. Hussin, D.M. Said, A review on lighting control technologies in commercial buildings, their performance and affecting factors, *Renew. Sustain. Energy Rev.* 33 (2014) 268–279.
- [27] L. Bellia, F. Fragliasso, G. Riccio, Daylight fluctuations effect on the functioning of different daylight-linked control systems, *Build. Environ.* 135 (2018) 162–193.
- [28] S.-Y. Kim, J.-J. Kim, Influence of light fluctuation on occupant visual perception, *Build. Environ.* 42 (8) (2007) 2888–2899.
- [29] Arduino. Technical Data. Available from: <http://www.arduino.cc/en/Main/ArduinoBoardMini> (Accessed on: 6 June 2018).
- [30] DIGI. Technical Data. Available from: <https://www.digi.com> (Accessed on: 6 June 2018).
- [31] F. Leccese, Remote-control system of high efficiency and intelligent street lighting using a ZigBee network of devices and sensors, *IEEE Trans. Power Deliv.* 28 (2013) 21–28.
- [32] K. Lappalainen, S. Valkealahti, Recognition and modelling of irradiance transitions caused by moving clouds, *Sol. Energy* 112 (2015) 55–67.
- [33] M. Lave, M.J. Reno, R.J. Broderick, Characterizing local high-frequency solar variability and its impact to distribution studies, *Sol. Energy* 118 (2015) 327–337.
- [34] K. Lappalainen, S. Valkealahti, Apparent velocity of shadow edges caused by moving clouds, *Sol. Energy* 138 (2016) 47–52.
- [35] G.O. Schlegel, F.W. Burkholder, S.A. Klein, W.A. Beckman, B.D. Wood, J.D. Muhs, Analysis of a full spectrum hybrid lighting system, *Sol. Energy* 76 (2004) 359–368.
- [36] Y. Liu, J. Yang, Y. Lin, H. Lv, Research on medical applications of contrast sensitivity function to red–green gratings in 3D space, *Neurocomputing* 220 (2017) 34–40.
- [37] Y.-Y. Liao, S.-C. Tai, J.-S. Lin, P.-J. Liu, Degradation of turbid images based on the adaptive logarithmic algorithm, *Comput. Math. Appl.* 64 (2012) 1259–1269.
- [38] IESNA, *Lighting Design Guide in the IESNA Lighting Handbook. Reference & Application*, ninth ed., Mark S. Rea, New York, 2000.
- [39] T. Kimpe, T. Tuyschaever, Increasing the number of gray shades in medical display systems-how much is enough, *J. Digit. Imag.* 20 (4) (2007) 422–432.
- [40] N. Gentile, T. Laike, M.-C. Dubois, Lighting control systems in individual offices rooms at high latitude: measurements of electricity savings and occupants' satisfaction, *Sol. Energy* 127 (2016) 113–123.
- [41] P.R. Boyce, J.A. Veitch, G.R. Newsham, C.C. Jones, J. Heerwagen, M. Myer, C.M. Hunter, Occupant use of switching and dimming controls in offices, *Light. Res. Technol.* 38 (2006) 358–376.
- [42] P.R. Boyce, *Human Factors in Lighting*, third ed., CRC Press, 2014.
- [43] J.A. Duffie, W.A. Beckman, *Solar Engineering of Thermal Processes*, fourth ed., John Wiley & Sons, New York, 2013.
- [44] V.M. Sharma, J.K. Nayak, S.B. Kedare, Comparison of line focusing solar concentrator fields considering shading and blocking, *Sol. Energy* 122 (2015) 924–939.
- [45] INGLASS. Technical Data. Available from: <http://www.inglass.es/en/> (Accessed on: 2 January 2019).
- [46] EN 12464-1:2003, *Light and Lighting- Lighting of Work Places- Part 1, Indoor Work Places*, 2003.
- [47] T. Muneer, *Solar Radiation and Daylight Models*, Elsevier Butterworth - Heinemann, Oxford, 2004.
- [48] K.K. Chong, N.O. Onubogu, T.K. Yew, C.W. Wong, W.C. Tan, Design and construction of active daylighting system using two-stage non-imaging solar concentrator, *Appl. Energy* 207 (2017) 45–60.
- [49] Thorlabs. Technical Data. Available from: <https://www.thorlabs.com/> (Accessed on: 8 January 2019).
- [50] Andalusian Energy Agency (AEA). <https://www.agenciaandaluzadelaenergia.es/Radiacion/radiacion1.php>.